Exploiting Cannabinoid-Induced Cytotoxic Autophagy to Drive Melanoma Cell Death

Jane L. Armstrong[1,2], David S. Hill[1], Christopher S. McKee[1], Sonia Hernandez-Tiedra[3], Mar Lorente[3], Israel Lopez-Valero[3,4], Maria Eleni Anagnostou[1], Fiyinfoluwa Babatunde[1], Marco Corazzari[5], Christopher P.F. Redfern[6], Guillermo Velasco[3,4,7] and Penny E. Lovat[1,7]

Although the global incidence of cutaneous melanoma is increasing, survival rates for patients with metastatic disease remain <10%. Novel treatment strategies are therefore urgently required, particularly for patients bearing BRAF/NRAS wild-type tumors. Targeting autophagy is a means to promote cancer cell death in chemotherapy-resistant tumors, and the aim of this study was to test the hypothesis that cannabinoids promote autophagy-dependent apoptosis in melanoma. Treatment with Δ^9-Tetrahydrocannabinol (THC) resulted in the activation of autophagy, loss of cell viability, and activation of apoptosis, whereas cotreatment with chloroquine or knockdown of Atg7, but not Beclin-1 or Ambra1, prevented THC-induced autophagy and cell death in vitro. Administration of Sativex-like (a laboratory preparation comprising equal amounts of THC and cannabidiol (CBD)) to mice bearing BRAF wild-type melanoma xenografts substantially inhibited melanoma viability, proliferation, and tumor growth paralleled by an increase in autophagy and apoptosis compared with standard single-agent temozolomide. Collectively, our findings suggest that THC activates noncanonical autophagy-mediated apoptosis of melanoma cells, suggesting that cytotoxic autophagy induction with Sativex warrants clinical evaluation for metastatic disease.

INTRODUCTION

Cutaneous melanoma incidence continues to increase, and response rates of patients with metastatic melanoma to current therapy remain poor (Garbe et al., 2011). Identification of driver mutations and development of targeted therapies to BRAF/MEK have revolutionized melanoma therapy, although clinical resistance is inevitable (Chen and Davies, 2014). The emergence of immunotherapies that are able to promote tumor T-cell responses is further changing melanoma management (Wolchok et al., 2010); however, not all patients respond (Prieto et al., 2012). It is therefore clear that there is no consistently beneficial treatment for metastatic melanoma and alternative approaches should be explored.

Autophagy (macroautophagy) is the principal lysosomal-mediated mechanism for the degradation of damaged or long-lived organelles and proteins. Under physiological conditions, autophagy maintains normal turnover of cellular components, as well as responding to metabolic stress, whereas in pathological settings autophagy activation mediates defense against extracellular insults and pathogens (Choi et al., 2013). The current model for the role of autophagy in cancer is that in the early stages of tumor development, quality control by autophagy inhibits tumorigenesis, whereas in advanced cancer autophagy provides energy to meet the increased demands and a means to resist cell death caused by cytotoxic therapy (White, 2012). Preclinical data suggest that lysosomal inhibition can cause tumor regression, and the lysosome inhibitors chloroquine or hydroxychloroquine are now being evaluated in clinical trials either alone or in combination with chemotherapy (Yang et al., 2011). However, recent studies suggest that chloroquine/hydroxychloroquine treatment may promote tumor development (Michaud et al., 2011; Maycotte et al., 2012), questioning the benefit of autophagy inhibition. An alternative approach for autophagy modulation is via exacerbation; although initially this appears counterintuitive to treat advanced cancer, recent evidence suggests that in particular circumstances a consequence of autophagy activation is cell death (Ding et al., 2007; Scarlatti

et al., 2008; Tomic *et al.*, 2011; Basit *et al.*, 2013). Therapeutic exploitation of cytotoxic autophagy to drive cancer cell death is therefore an emerging concept for the development of novel cancer treatments.

Cannabinoids are a diverse class of compounds derived from *Cannabis sativa*, with Δ^9-tetrahydrocannabinol (THC) the most relevant owing to its high potency and abundance (Pertwee, 2008). THC exerts its biological effects by mimicking endocannabinoids that bind to and activate two G protein–coupled cannabinoid receptors: CB1 and CB2 (Howlett *et al.*, 2002). CB1/CB2 receptors are expressed in many cancer cell types (Velasco *et al.*, 2012), and cannabinoids are currently being investigated as anticancer agents, including glioblastoma for which THC has shown considerable promise (Velasco *et al.*, 2012). Preclinical data demonstrate that THC exerts its antitumoral action via induction of endoplasmic reticulum (ER) stress, upregulation of the transcriptional coactivator p8 and the pseudo-kinase tribbles homolog 3 (TRIB3), the stimulation of autophagy, and execution of apoptosis (Carracedo *et al.*, 2006; Salazar *et al.*, 2009a, b). Blockade of autophagy prevents THC-induced apoptosis and cell death, indicating that autophagy is upstream of apoptosis and demonstrating the potential of p8/TRIB3-mediated autophagy as a cytotoxic pathway.

Alongside genetic changes, adaption to ER stress and the aberrant control of autophagy have emerged as key drivers of malignancy and therapy resistance in advanced melanoma (Armstrong *et al.*, 2011; Corazzari *et al.*, 2013). The cannabinoid receptors have previously been identified as potential therapeutic targets (Blazquez *et al.*, 2006; Carracedo *et al.*, 2006); hence, targeting ER stress responses combined with cytotoxic autophagy using cannabinoids may represent a valuable therapeutic approach for metastatic melanoma. The aim of this study was to determine whether THC activates cytotoxic autophagy in melanoma cells *in vitro* and *in vivo*. Our data suggest a noncanonical mechanism of autophagy-mediated apoptosis, highlighting the potential to harness autophagy for therapeutic benefit in advanced melanoma.

RESULTS

THC activates autophagy and apoptosis in melanoma cells

Characteristic features of early and late stages of autophagy were assessed using LC3 lipidation (LC3-II) and analysis of autophagic flux using chloroquine and visualization of
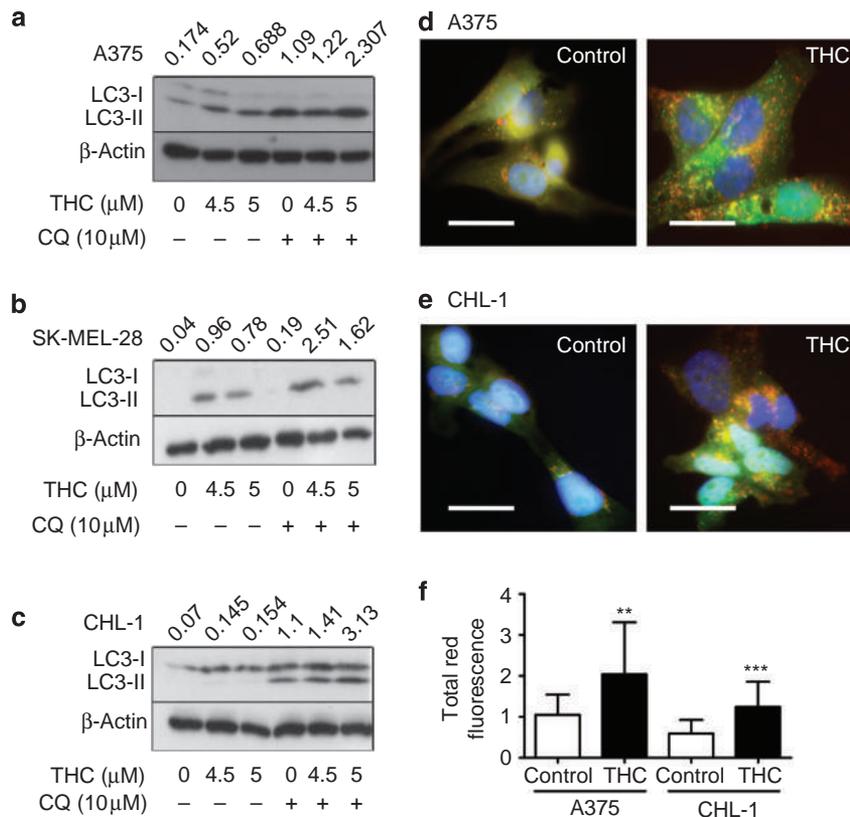

Figure 1. The Δ^9-Tetrahydrocannabinol (THC) induces autophagy in melanoma cells. (**a–c**) A375, SK-MEL-28, and CHL-1 cells were treated with vehicle or THC (4.5 or 5 μM) for 24 hours in the presence or absence of chloroquine (CQ; 10 μM) for the final 2 hours, and LC3 and β-actin expression was determined by western blotting. LC3-II expression was quantified and band intensity normalized to β-actin. Data are expressed as fold change relative to the mean LC3-II/β-actin value for a representative experiment and are shown above the western blot (representative data from $n=3$ independent experiments). (**d**, **e**) mRFP–GFP–LC3 expressing (**d**) A375 or (**e**) CHL-1 cells were treated with vehicle or THC (4.5 μM) for 18 hours. Data are representative fluorescent micrographs (bar = 20 μm) of three independent experiments. (**f**) Total red fluorescence values were generated from ≥ 20 cells per treatment condition, from two independent experiments. Pixel intensities were divided by a factor of 10^6, and data are shown as mean ± SD (**$P<0.01$ and ***$P<0.001$ vs. control for each cell line). mRFP–GFP, monomeric red fluorescent protein–green fluorescent protein.
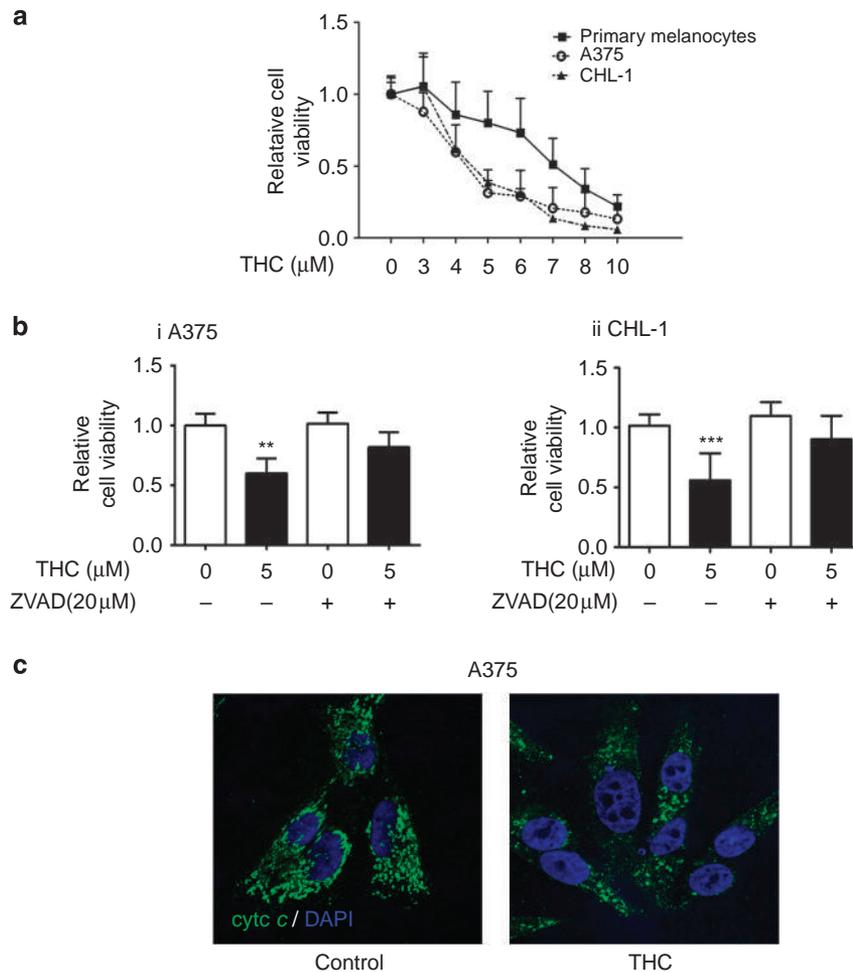
Figure 2. The Δ⁹-Tetrahydrocannabinol (THC) induces apoptosis of melanoma cells. (**a**) Primary melanocytes, A375, and CHL-1 cells were treated with vehicle or THC (3–10 μM) for 24 hours. (**b**) A375 (i) or CHL-1 (ii) cells were treated with vehicle or THC (5 μM) in the presence or absence of ZVAD (20 μM) for 24 hours. Cell viability was determined by the 3-(4,5-dimethylthiazol-2-yl)-2,5-diphenyltetrazolium bromide (MTT) assay. Data generated in triplicate were expressed relative to the mean of vehicle-treated cells in each experiment, for three independent experiments, and shown as mean ± SD (t-test; **P < 0.01 and ***P < 0.001 vs. THC+ZVAD). (**c**) A375 cells were treated with THC (5 μM) for 24 hours. Data are representative fluorescent micrographs of cytochrome *c* immunostaining (bar = 20 μm) of three independent experiments.

tandem mRFP–GFP (monomeric red fluorescent protein–green fluorescent protein)–tagged LC3 (Kimura *et al.*, 2007), respectively. LC3-II induction was observed in three human melanoma cell lines in response to THC, and LC3-II accumulated further in the presence of chloroquine in both BRAF wild-type (CHL-1) and mutated (A375 and SK-MEL-28) melanoma cells. In addition, increased numbers of LC3-positive autophagosomes (yellow puncta) and autolysosomes (red puncta) and total red fluorescence (CHL-1: $t_{43} = 4.17$, $P < 0.001$; A375: $t_{42} = 3.289$, $P = 0.002$) were observed in A375 and CHL-1 cells in response to THC treatment, indicating activation of autophagic flux (Figure 1).

THC reduced melanoma cell viability in a dose-dependent manner while having little effect on primary melanocytes at doses up to 6 μM THC (Figure 2a). Cotreatment of melanoma cells with submaximal concentrations of THC and the pan-caspase inhibitor ZVAD-fmk significantly increased cell viability compared with treatment with THC alone (CHL-1:

$t_{22} = 3.962$, $P = 0.0007$; A375: $t_{16} = 3.74$, $P = 0.0018$; Figure 2b), suggesting that cell death is caspase dependent. In addition, the cytochrome *c*–labeled structures present in vehicle-treated cells were substantially reduced in THC-treated cells (Figure 2c), indicating apoptosis activation.

THC-induced apoptosis is dependent on autophagy
In glioma, THC activates apoptosis via a mechanism involving TRIB3 and Beclin-1-dependent autophagy (Carracedo *et al.*, 2006; Salazar *et al.*, 2009b). The small interfering RNA (siRNA)-mediated knockdown of TRIB3 significantly prevented loss of cell viability in response to THC in A375 cells (one-way analysis of variance (ANOVA); $F_{5, 48} = 5.053$, $P = 0.001$; THC compared with vehicle treatment in siCtrl cells; Tukey's $P < 0.05$; Supplementary Figure S1 online), demonstrating that TRIB3 mediates THC-induced cell death. Furthermore, siRNA-mediated knockdown of Atg7 prevented THC-induced accumulation of LC3-II in the presence of

chloroquine (one-way ANOVA; $F_{11, 24} = 6.878$, $P < 0.001$; chloroquine compared with chloroquine+THC-treated siCtrl cells contrast $P < 0.05$; Figure 3a and b). THC-induced caspase 3 cleavage was also inhibited by Atg7 knockdown in A375 (Figure 3a), as well as in CHL-1 and SK-MEL-28 cells (CHL-1: one-way ANOVA; $F_{5, 12} = 6.57$, $P = 0.004$; THC compared with vehicle-treated siCtrl cells; Tukey's $P < 0.05$; SK-MEl-28: one-way ANOVA; $F_{3, 8} = 4.646$, $P = 0.037$; THC compared with vehicle-treated siCtrl cells; Tukey's $P < 0.05$; Supplementary Figure S2 online). In addition, THC treatment resulted in a significant loss of melanoma cell viability only in the absence of chloroquine or Atg7 siRNA (Figure 3 and Supplementary Figure S2 online; *post hoc* tests, Games–Howell, or Tukey's $P < 0.01$). In A375 and SK-MEL-28 cells, knockdown of Atg7 alone had no effect on cell viability; however, in CHL-1 cells, downregulation of Atg7 resulted in a significant loss of cell viability (Tukey's $P < 0.001$; Supplementary Figure S2a online), suggesting that basal autophagy is required to maintain viability in these cells. Collectively, these data demonstrate that THC-induced apoptosis of melanoma cells requires TRIB3 and is mediated by Atg7-dependent autophagy.

Beclin-1 promotes autophagy induction and autophagosome formation (Russell *et al.*, 2013); however, Beclin-1-independent autophagy has been reported (Scarlatti *et al.*, 2008; Grishchuk *et al.*, 2011). Unlike in glioma cells, Beclin-1 knockdown did not prevent THC-induced LC3-II accumulation or caspase 3 cleavage ($t_4 = 4.494$, $P = 0.011$; Supplementary Figure S3a online) in A375 cells (Figure 4a), and THC treatment resulted in a significant loss of cell viability under both control and Beclin-1 knockdown conditions (Welch ANOVA; $F_{5, 19.63} = 94.53$, $P < 0.001$; THC treatments compared with vehicle-treated shRNA cells; Games–Howell $P < 0.001$; Figure 4a i) and ii)). These results suggest that autophagy and subsequent apoptosis occur independently of Beclin-1. Furthermore, knockdown of the Beclin-1-interacting protein Ambra1 failed to prevent THC-induced LC3-II induction and caspase 3 cleavage ($t_4 = 6.097$, $P = 0.004$; Supplementary Figure S3b online and Figure 4b). The effect of Ambra1 knockdown alone on A375 viability was variable; however, THC treatment resulted in a significant loss of cell viability under both control ($t_{16} = 9.44$, $P < 0.001$) and Ambra1 knockdown conditions ($t_{16} = 10.61$, $P < 0.001$) (Figure 4biii). Collectively, these data suggest that THC activates noncanonical autophagy-mediated apoptosis of melanoma cells that is dependent on Atg7 but not Beclin-1 or Ambra1.

Cannabinoid treatment stimulates autophagy and apoptosis and the abrogation of melanoma growth *in vivo*
A 1:1 mixture of submaximal doses of THC–botanical drug substance (BDS) and the nonpsychoactive cannabinoid cannabidiol (CBD) –BDS, a laboratory mimic of the clinical cannabinoid Sativex (Sat-L) (an oromucosal spray of standardized cannabis extract comprising equal amounts of THC and CBD (GW Pharmaceuticals)), reduced glioma growth *in vivo* to the same extent as an identical dose of THC (Torres *et al.*, 2011). Treatment of melanoma cells with THC+CBD resulted in a substantial loss of melanoma cell viability at a
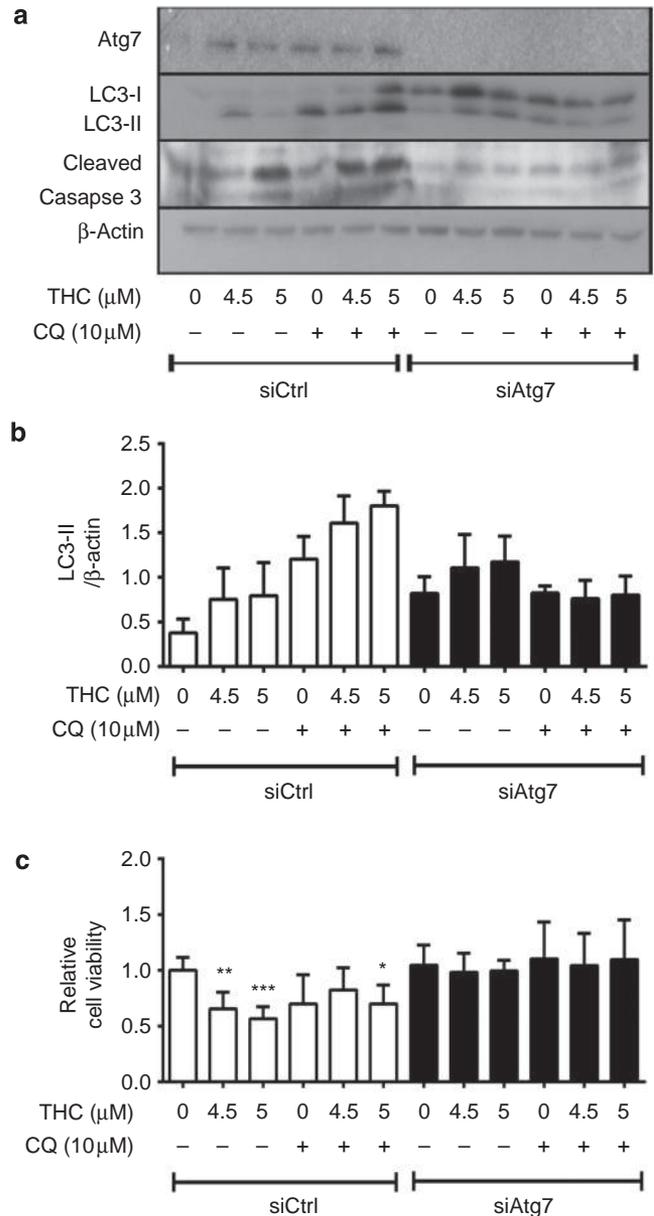
Figure 3. The Δ⁹-Tetrahydrocannabinol (THC)-induced apoptosis requires autophagy. (a–c) A375 cells were transfected with small interfering RNAs (siRNAs) for Atg7 (siAtg7) or with a nonsilencing control siRNA (siCtrl) before treatment with vehicle or THC (4.5, 5 μM) for 24 hours in the presence or absence of chloroquine (CQ; 10 μM) for the (a, b) final 2 hours or for (c) 24 hours. (a, b) Atg7, LC3, cleaved caspase 3, and β-actin expression were determined by western blotting. LC3-II expression was quantified and band intensity normalized to β-actin. Data are expressed as fold change relative to the mean LC3-II/β-actin value for each experiment, for three separate experiments (mean ± SD, n = 3). (c) Cell viability was determined by the 3-(4,5-dimethylthiazol-2-yl)-2,5-diphenyltetrazolium bromide (MTT) assay. Data generated in triplicate were expressed relative to the mean of vehicle-treated siCtrl cells in each experiment, for three independent experiments, and shown as mean ± SD (*P < 0.05, **P < 0.01, and ***P < 0.001 vs. vehicle-treated siCtrl cells).

concentration of 1 μM THC+1 μM CBD in CHL-1, A375, and SK-MEL-28 cells compared with equivalent concentrations of THC, whereas temozolomide had little effect (Figure 5). Temozolomide is an alkylating agent currently indicated as
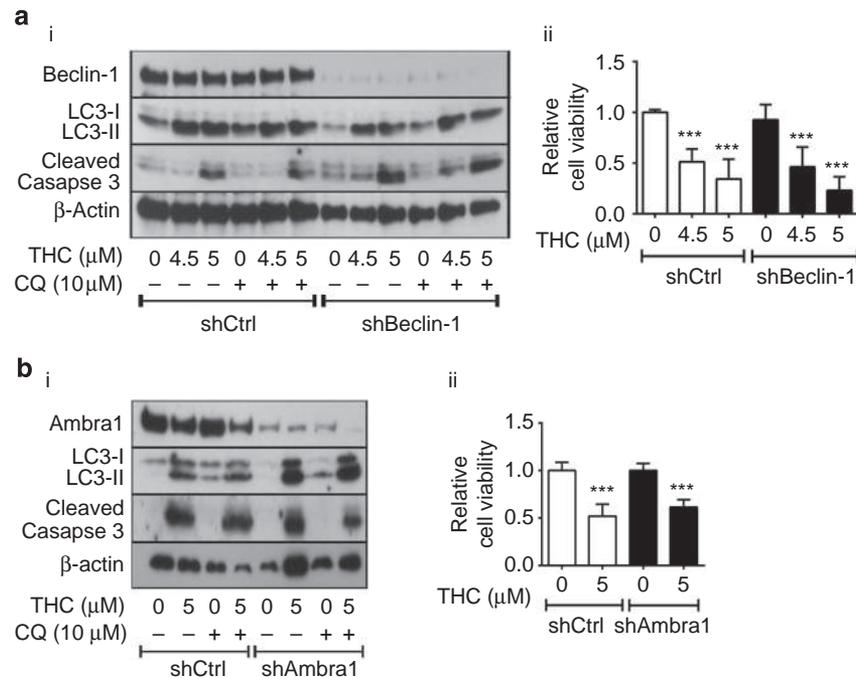
Figure 4. The Δ⁹-Tetrahydrocannabinol (THC)-induced autophagy and cell death is not dependent on Beclin-1 or Ambra1. (a) A375 cells stably expressing short hairpin RNA (shRNA) for Beclin-1 (shBeclin1) or a nonsilencing control shRNA (shCtrl) were treated with vehicle or THC (4.5 and 5 μM) for 48 hours in the presence or absence of chloroquine (CQ; 10 μM) for the final 2 hours (i). Beclin-1, LC3, cleaved caspase 3, and β-actin expression were determined by western blotting (i). Cell viability (ii) was determined by the 3-(4,5-dimethylthiazol-2-yl)-2,5-diphenyltetrazolium bromide (MTT) assay. Data generated in triplicate were expressed relative to the mean of vehicle-treated shCtrl cells in each experiment, for three independent experiments, and shown as mean ± SD (***$P < 0.001$ vs. vehicle-treated shCtrl cells). (b) A375 cells stably expressing shRNA for Ambra1 (shAmbra1) or a nonsilencing control shRNA (shCtrl) were treated with vehicle or THC (5 μM) for 24 hours in the presence or absence of CQ (10 μM) for the final 2 hours (i). Ambra1, LC3, cleaved caspase 3, and β-actin expression were determined by western blotting (i). Cell viability (ii) was determined by the MTT assay. Data generated in triplicate were normalized to the mean of vehicle-treated cells for each shRNA in each experiment, for three independent experiments, and shown as mean ± SD (***$P < 0.001$ vs. vehicle-treated cells for each shRNA).

standard single-agent chemotherapy for metastatic melanoma. The *in vivo* relevance of these findings was evaluated in the context of BRAF wild-type melanoma tumors, for which there is a particular demand for novel therapeutic approach in the absence of targeted therapies in this tumor group. CHL-1 xenograft tumors were treated for 20 days with temozolomide, THC, or Sativex-L. Both THC and Sativex-L significantly inhibited the growth of xenografts (one-way ANOVA; $F_{3,16} = 9.347$, $P = 0.001$; THC or Sat-L compared with vehicle, Sat-L compared with Temozolomide: $P < 0.05$, Figure 6a). Tumors removed from animals at the time of killing were processed for immunohistochemical analysis of proliferative activity (Ki67), apoptosis (TUNEL), and autophagy (LC3). Ki67 fluorescence differed significantly between drug treatments (Welch ANOVA; $F_{3,16.28} = 61.363$, $P < 0.001$; Figure 6b) and was significantly reduced in tumors from animals treated with temozolomide, THC, or Sativex-L compared with control animals (Games–Howell; $P \leq 0.001$), as well as in tumors from animals treated with THC or Sativex-L compared with those treated with temozolomide (Games–Howell; $P < 0.001$). TUNEL fluorescence also differed significantly between treatments (one-way ANOVA; $F_{3,32} = 13.31$, $P < 0.001$) and was higher than control in tumors from animals treated with THC or Sativex-L (Tukey's $P \leq 0.001$) and higher in tumors from animals treated with Sativex-L compared with those treated with temozolomide (Tukey's $P < 0.05$; Figure 6c).

Correspondingly, LC3 fluorescence differed between treatments (one-way ANOVA; $F_{3,32} = 3.539$, $P < 0.05$), with significantly increased LC3 staining in tumors from animals treated with Sativex-L compared with tumors from animals treated with vehicle or temozolomide (Tukey's $P \leq 0.05$, Figure 6d). Staining for Ki67, TUNEL, and LC3 was not significantly different in tumors from animals treated with THC compared with Sativex-L. Collectively, these data suggest that THC and Sativex-L are more effective than temozolomide in terms of apoptosis induction and antitumor response, further validating the therapeutic relevance of cannabinoid treatment for melanoma.

DISCUSSION

It is apparent that autophagy modulation may offer considerable benefit in cancer treatment; however, potential drawbacks to autophagy inhibition have recently been identified (Michaud et al., 2011; Maycotte et al., 2012; Takahashi et al., 2012; Rosenfeldt et al., 2013). Emerging evidence indicates that activation of autophagy can, in some circumstances, promote cell death; stimulation of cytotoxic autophagy therefore represents an alternative approach to autophagy modulation (Ding et al., 2007; Scarlatti et al., 2008; Salazar et al., 2009b; Grishchuk et al., 2011; Tomic et al., 2011; Basit et al., 2013). Here, we show that the cannabinoid THC exerts its antitumor effect on melanoma cells via activation of noncanonical
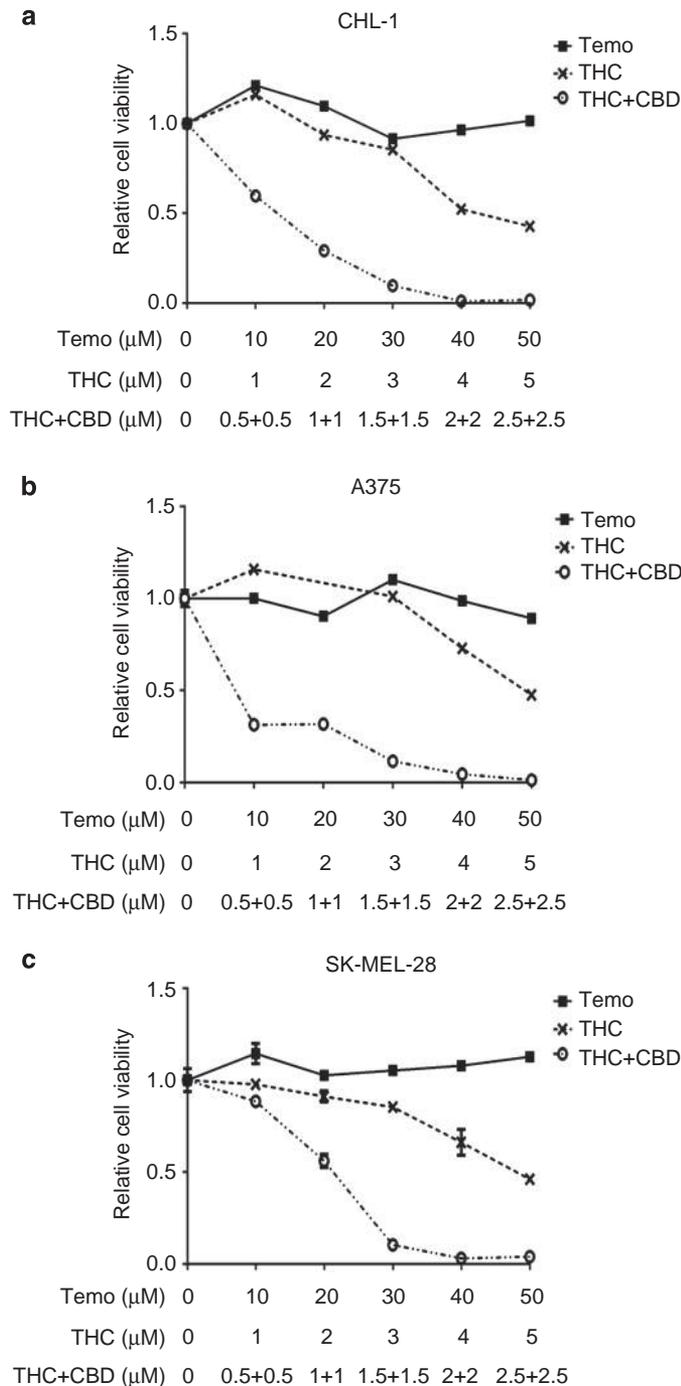
a

b

c

Figure 5. Cannabinoids inhibit melanoma cell viability *in vitro*. (**a–c**) CHL-1 (**a**), A375 (**b**), or SK-MEL-28 (**c**) cells were treated with temozolomide (Temo; 10–50 μM), Δ⁹-Tetrahydrocannabinol (THC; 1–5 μM), or THC+CBD (0.5 μM THC+0.5 μM CBD to 2.5 μM THC+2.5 μM CBD) for 48 hours. Cell viability was determined by the 3-(4,5-dimethylthiazol-2-yl)-2,5-diphenyltetrazolium bromide (MTT) assay. Data generated in triplicate were expressed relative to the mean of vehicle-treated cells for each drug treatment in each experiment, for three independent experiments, and shown as mean ± SD for a representative experiment. CBD, cannabidiol.

autophagy and subsequent apoptosis, suggesting that canna-binoids may be of clinical benefit for metastatic melanoma.

The molecular mechanisms connecting autophagy to cell death remain poorly understood (Shen and Codogno, 2011);

however, reports describing autophagy-dependent apoptosis (Ding *et al.*, 2007; Salazar *et al.*, 2009b; Grishchuk *et al.*, 2011; Tomic *et al.*, 2011) suggest multiple interactions between autophagic and apoptotic machinery. THC exerts its effect via the *de novo* synthesis of the sphingolipid cera-mide, leading to the activation of ER stress, TRIB3-dependent inhibition of Akt/mTORC1 signaling, and autophagy-mediated apoptosis (Carracedo *et al.*, 2006; Salazar *et al.*, 2009b). TRIB3 has been identified as a key switch between cell survival and apoptosis during stress responses (Shimizu *et al.*, 2012), and the participation of TRIB3 in the melanoma response to THC may direct cellular fate toward apoptosis in the context of ER stress–induced autophagy (Salazar *et al.*, 2013).

Autophagy inhibition using both molecular and pharmaco-logical approaches prevented THC-induced autophagy and apoptosis of melanoma cells. However, THC-induced autop-hagy was not prevented by knockdown of Beclin-1, suggest-ing that, in contrast to glioma, noncanonical autophagy mediates apoptosis in response to THC in melanoma. Beclin-1-independent autophagy may promote caspase-independent cell death (Scarlatti *et al.*, 2008; Basit *et al.*, 2013) as well as apoptosis (Grishchuk *et al.*, 2011; Tomic *et al.*, 2011), suggesting that autophagy mechanisms not involving Beclin-1 exist that interact with cell death machinery. Interest-ingly, in contrast to previous studies (Salazar *et al.*, 2009b), THC-induced autophagy was also independent of Ambra1 in melanoma cells. Ambra1 is a Beclin-1 interacting protein that promotes autophagy by stabilizing Beclin-1 complexes (Fimia *et al.*, 2007); although supporting the concept of Beclin-1-independent autophagy activation in response to THC, these data highlight the complex regulation of autophagy that likely occurs in a cell type- and context-specific manner.

Tumor-selective killing can be achieved by targeting pathways that are differentially regulated in cancer cells compared with normal cells. In this respect, we have shown that normal human melanocytes are resistant to THC at concentrations that cause cell death in melanoma cells. This is consistent with studies showing that cancerous cells are more sensitive to THC and other cannabinoid receptor ligands compared with their nontransformed counterparts, despite the presence of functional CB receptors (Velasco *et al.*, 2012). Together with previous studies demonstrating an effect of synthetic ligands of cannabinoid receptors in melanoma (Blazquez *et al.*, 2006), these data support clinical evaluation of cannabinoids in advanced-stage disease. Furthermore, THC activates autophagy and apoptosis in both BRAF wild-type and mutated melanoma cell lines, suggesting that despite autophagy deregulation (Armstrong *et al.*, 2011; Corazzari *et al.*, 2013), THC is likely effective in melanoma tumors regardless of BRAF mutation status. Furthermore, our findings show that THC is able to reduce melanoma cell viability and tumor xenograft growth alone, but when lower doses of THC are combined with CBD the antitumor effect was enhanced *in vitro* and was at least equally effective as the higher dose of single-agent THC *in vivo*. Moreover, CBD induces apoptosis via the production of reactive oxygen species and caspase activation in cancer cells (Massi *et al.*, 2006; Shrivastava *et al.*, 2011), indicating that THC and CBD engage different
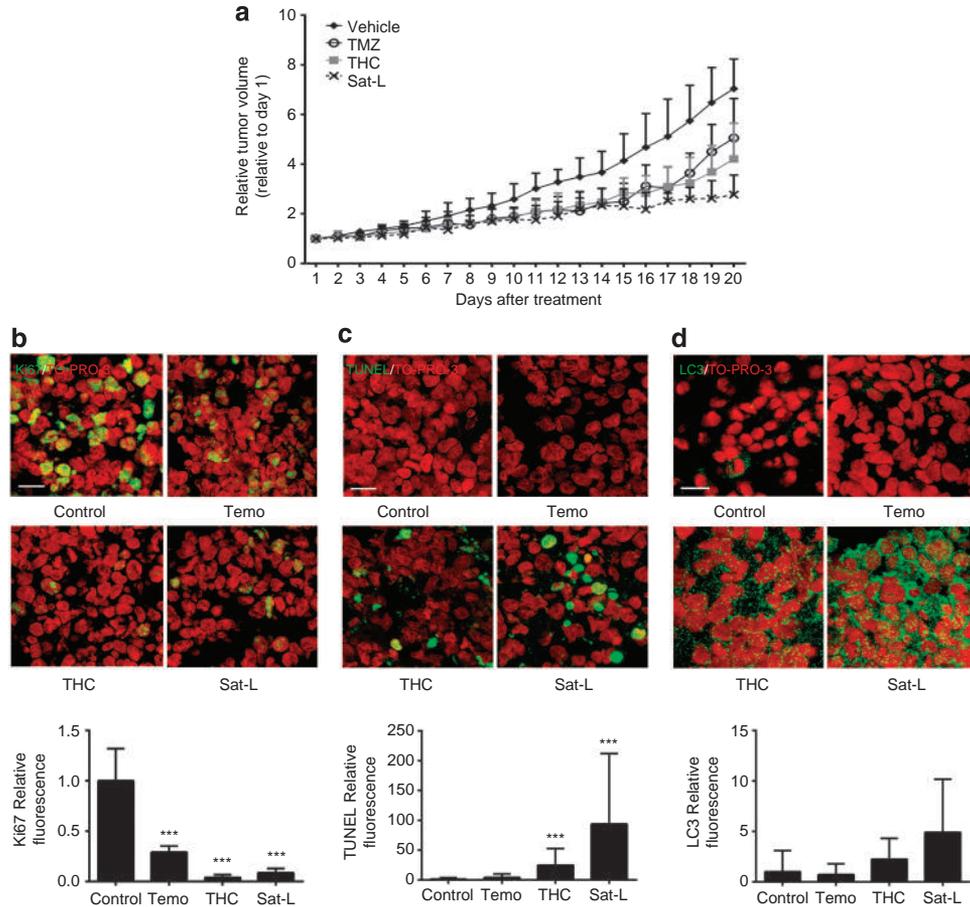
Figure 6. The Δ⁹-Tetrahydrocannabinol (THC) and Sativex-like cannabinoids promote autophagy and antitumor responses in melanoma xenografts. Athymic nude mice were injected subcutaneously in the right flank with CHL-1 melanoma cells. When tumors reached a 250 mm³ size, mice were treated daily for 20 days with vehicle, temozolomide (TMZ; 5 mg kg⁻¹; local administration), THC (15 mg kg⁻¹; oral administration), or Sativex-like (Sat-L; 7.5 mg kg⁻¹ THC–BDS+7.5 mg kg⁻¹ CBD–BDS; oral administration). (**a**) Tumor volumes were measured daily. Each point is the mean from ≥5 tumors ± SD and is expressed relative to the tumor volume on day 1 of treatment. (**b–d**) Immunohistochemical analysis of CHL-1 xenograft tumors treated with temozolomide, THC, or Sat-L. (**b–d**) Micrographs of tumor sections stained for (**b**) Ki67, (**c**) TUNEL, or (**d**) LC3. In each, green is staining for Ki67, TUNEL, or LC3, and red is the TO-PRO-3 counterstain. The bar graphs below each set of micrographs summarize the data analysis from tumor sections (bar = 20 μm). Total fluorescence values (total fluorescence (LC3/Ki67/TUNEL)/total nuclear fluorescence) were generated in triplicate for 3 tumors in each treatment group. Data are expressed as fold change relative to the mean value obtained from control animals, from two independent staining analyses, and shown as mean ± SD (**P < 0.01 and ***P < 0.001 vs. control animals).

molecular machineries that cooperate to promote tumor cell death (Shrivastava *et al.*, 2011; Torres *et al.*, 2011).

In summary, these data highlight the potential for cannabinoid-induced cytotoxic autophagy as an effective strategy to drive melanoma cell death, supporting the clinical evaluation of Sativex for the treatment of metastatic disease.

MATERIALS AND METHODS
Cell culture, viability assays, and drug treatment
Melanoma cell lines CHL-1, A375, and SK-MEL-28 were obtained from the ATCC (Manassas, VA) in 2006 and cultured as described previously (Armstrong *et al.*, 2007). Cell lines were verified by melan A staining (Flockhart *et al.*, 2009) with *B-RAF/NRAS* mutational status confirmed using Custom TaqMan SNP genotyping assays (Hiscutt *et al.*, 2010) (Applera Europe BV, Life Technologies, Paisley, UK) (last tested February 2014). Before drug treatment, culture medium was changed to 0.5% fetal bovine serum medium. Temozolomide (OSI

Pharmaceuticals, Melville, NY) and ZVAD-fmk (benzyloxycarbonyl-V-A-D(OMe)-fluoromethylketone) (Tocris Bioscience, Bristol, UK) were added in DMSO, and chloroquine (Sigma-Aldrich Ltd, Poole, UK) was added in water. For *in vitro* experiments, pure THC (THC Pharm, Frankfurt, Germany) and CBD (synthesized by Professor Raphael Mechoulam (Hebrew University of Jerusalem) and kindly provided by Dr Javier Fernandez Ruiz (Complutense University, Madrid, Spain)) were prepared in DMSO. Control incubations contained the same amount of DMSO (0.1–0.2% v/v). For treatment with THC+CBD, pure THC and pure CBD were mixed 1:1 (w/w). Analysis of cell viability was performed using 3-(4,5-dimethylthiazol-2-yl)-2,5-diphenyltetrazolium bromide (MTT; Sigma). For *in vivo* experiments, THC–BDS (THC content 67.6% w/w; CBD content 0.3% w/w; other individual plant cannabinoids <1.5% w/w) and CBD–BDS (CBD content 65.4% w/w; THC content 2.5% w/w; other individual plant cannabinoids <1.7% w/w) were provided by GW Pharmaceuticals (Cambridge, UK). THC–BDS and CBD–BDS were provided as a resin, dissolved in ethanol (100

mg ml^{-1}), dried, and prepared in DMSO. A 1:1 (w/w) preparation of THC–BDS and CBD–BDS was used to mimic Sativex (Sat-L). For oral administration, THC or Sat-L was solved in 100 μl of sesame oil.

Western blotting and reverse transcription–PCR analysis

Preparation of whole-cell lysates and western blotting for LC3B, cleaved caspase 3 (Cell Signaling Technology, Leiden, The Netherlands), Atg7 (Santa Cruz Biotechnology, Heidelberg, Germany), Beclin-1 (BD Biosciences, Oxford, UK), and Ambra1 (Novus Biologicals, Cambridge, UK) all diluted 1:4,000, and β-actin (Sigma) diluted 1:30,000, were performed as described previously (Armstrong *et al.*, 2007). Total RNA was isolated from cells using the RNeasy Mini Kit with DNase digestion (Qiagen, Manchester, UK) according to the manufacturer's protocol. Reverse transcription–PCR was performed using the Access Reverse transcription–PCR system (Promega, Southampton, UK) using primers for TRIB3 (Carracedo *et al.*, 2006) or β-actin (Armstrong *et al.*, 2005). PCR products were analyzed by electrophoresis on ethidium bromide–stained 2% agarose gels and DNA visualized by exposure to UV light.

siRNA transfections

The siRNA for Atg7 (HSS116182), TRIB3 (sc-44426, Santa Cruz Biotechnology), or a nontargeting siRNA (Negative control Low GC Stealth RNAi) (Stealth RNAi, Life Technologies, Paisley, UK) were transfected into cells in OPTIMEM containing siRNA (2–4 nM) using Lipofectamine RNAiMAX (Life Technologies) according to the manufacturer's specification for reverse transfection. After 24 hours, the medium was replaced with DMEM containing 0.5% fetal bovine serum and cells treated with drugs as appropriate.

Retroviral or lentiviral infection

Retroviral expression of mRFP–GFP–LC3 (provided by T Yoshimori, Osaka University, Osaka, Japan) (Kabeya *et al.*, 2000; Kimura *et al.*, 2007) was performed as described previously (Armstrong *et al.*, 2011). Lentiviral expression of shAmbra1 or a nontargeting sequence shCtrl (MISSION shRNA, Sigma) was performed by cotransfection of 7.5 μg lentivirus vector (pLKO.1-puro) with 2.5 μg of an expression plasmid for the vesicular stomatitis virus G protein into 293 cells using the calcium precipitation method. After 48 hours, melanoma cells were incubated with virus-containing supernatant supplemented with polybrene (4 μg ml^{-1}) for 6–8 hours and selected for puromycin resistance. Lentiviral expression of shBeclin-1 (V3LHS_349509, Dharmacon, Chalfont St Giles, UK) or a nontargeting sequence shCtrl (RHS4346, Dharmacon) was performed by cotransfection of 20 μg lentivirus vector with 5 μg of an expression plasmid for the viral envelope (pMD2.G) and 15 μg packaging plasmid (pCMVdelta8.91) into HEK293T cells using the calcium precipitation method. After 72 hours, melanoma cells were spin transduced (1.5 hours, 1,200 r.p.m., Harrier 15/80, DJB Labcare, Newport Pagnell, UK) with virus-containing supernatant supplemented with polybrene (4 μg ml^{-1}) and selected for puromycin resistance.

Confocal microscopy

Cells were grown on glass coverslips before fixation in 4% paraformaldehyde. For immunolabeling, cells were incubated with 0.2% Triton X-100 before incubation with anti-cytochrome *c* (BD Biosciences) at room temperature for 1 hour (McGill *et al.*, 2005). Secondary labeling was performed with Oregon Green 488 conjugated to anti-rabbit IgG (Life Technologies). Nuclei were counterstained with TO-PRO-3 iodide (Life Technologies). Cells were imaged under a Leica TCS SP II laser-scanning confocal microscope with LCS Lite 2.61 software (Leica Microsystems, Milton Keynes, UK), using a 63 × oil objective.

Xenograft mouse model and immunohistochemical analysis

Athymic nude (nu/nu) 5-week-old male mice (Harlan Iberica Laboratory, Madrid, Spain) were inoculated by subcutaneous injection of 7.5×10^6 CHL-1 cells in 100 μl phosphate-buffered saline containing 0.1% glucose. On establishment of tumors 250 mm^3 in volume, mice were randomized into four treatment groups (5–8 mice per group) and treated by daily administration for 20 days with temozolomide (5 mg kg^{-1}, local peritumoral injection), THC (15 mg kg^{-1}, oral gavage), or Sativex (7.5 mg kg^{-1} THC–BDS+7.5 mg kg^{-1} CBD–BDS, oral gavage). The control group was treated with 100 μl of vehicle (sesame oil). Caliper measurements of tumor length (*l*) and width (*w*) were taken each day, and tumor volume was calculated as $(4\pi/3) \times (w/2)^2 \times (l/2)$. Mice were humanely killed on the final day of treatment, and tumors extracted and snap frozen in liquid nitrogen before storage at −80 °C. Frozen sections (6 μm) prepared on (3-Aminopropyl)triethoxysilane (Sigma)-coated glass slides were fixed in 4% paraformaldehyde before staining by TUNEL or with a Ki67 antibody (ab-15580, Abcam, Cambridge, UK) as previously described (Hill *et al.*, 2009). For LC3 immunolabeling, frozen sections were fixed in acetone and incubated with anti-LC3B (ab48394, Abcam) for 1 hour at room temperature. Secondary labeling was performed with Oregon Green 488 conjugated to anti-rabbit IgG (Life Technologies). Cells were imaged under a Leica TCS SP II laser-scanning confocal microscope with LCS Lite 2.61 software (Leica Microsystems), using a 63 × oil objective. All procedures involving animals were performed according to Spanish and European regulations and were approved by the ethical committee for animal experimentation from Complutense University.

Statistical analysis

Images of LC3, Ki67, and TUNEL staining were analyzed using Velocity (v4.3.1) (Improvision, Perkin Elmer, Coventry, UK). Total fluorescence was obtained by multiplying pixel number to the mean pixel intensity, after appropriate thresholding. TOPRO-3 fluorescence was determined by the number of pixels with fluorescence above the threshold, which was proportional to nuclei number. For each tumor (three animals per group, three randomly selected images each), values were reported as normalized total fluorescence (total fluorescence (LC3/Ki67/TUNEL)/total nuclear fluorescence) and expressed as fold change relative to the mean value obtained from control animals, from two independent staining analyses. The mRFP fluorescence was analyzed using ImageJ (public domain licence, http://imagej.nih.gov/ij/); data are total pixel intensities/cell minus the mean background fluorescence of nuclei. Homogeneity of variances was checked using Levene's test, and if variances were equal (normalized data or after log transformation) data were analyzed by drug treatment using Student's *t*-test or one-way ANOVA with planned contrasts (LC3 expression) or Tukey's *post hoc* test for multiple pairwise comparisons. Where variances were not equal, Welch ANOVA test was used with Games–Howell *post hoc* tests for pair-wise comparisons (SPSS Statistics 20, SPSS, IBM, Portsmouth, UK).

SUPPLEMENTARY MATERIAL

Supplementary material is linked to the online version of the paper at http://www.nature.com/jid

REFERENCES

Armstrong JL, Corazzari M, Martin S *et al.* (2011) Oncogenic B-RAF signaling in melanoma impairs the therapeutic advantage of autophagy inhibition. *Clin Cancer Res* 17:2216–26

Armstrong JL, Ruiz M, Boddy AV *et al.* (2005) Increasing the intracellular availability of all-trans retinoic acid in neuroblastoma cells. *Br J Cancer* 92: 696–704

Armstrong JL, Veal GJ, Redfern CP *et al.* (2007) Role of Noxa in p53-independent fenretinide-induced apoptosis of neuroectodermal tumours. *Apoptosis* 12:613–22

Basit F, Cristofanon S, Fulda S (2013) Obatoclax (GX15-070) triggers necroptosis by promoting the assembly of the necrosome on autophagosomal membranes. *Cell Death Differ* 20:1161–73

Blazquez C, Carracedo A, Barrado L *et al.* (2006) Cannabinoid receptors as novel targets for the treatment of melanoma. *FASEB J* 20:2633–5

Carracedo A, Lorente M, Egia A *et al.* (2006) The stress-regulated protein p8 mediates cannabinoid-induced apoptosis of tumor cells. *Cancer Cell* 9:301–12

Chen G, Davies MA (2014) Targeted therapy resistance mechanisms and therapeutic implications in melanoma. *Hematol Oncol Clin North Am* 28:523–36

Choi AM, Ryter SW, Levine B (2013) Autophagy in human health and disease. *N Engl J Med* 368:651–62

Corazzari M, Fimia GM, Lovat P *et al.* (2013) Why is autophagy important for melanoma? Molecular mechanisms and therapeutic implications. *Sem Cancer Biol* 23:337–43

Ding WX, Ni HM, Gao W *et al.* (2007) Differential effects of endoplasmic reticulum stress-induced autophagy on cell survival. *J Biol Chem* 282: 4702–10

Fimia GM, Stoykova A, Romagnoli A *et al.* (2007) Ambra1 regulates autophagy and development of the nervous system. *Nature* 447:1121–5

Flockhart RJ, Armstrong JL, Reynolds NJ *et al.* (2009) NFAT signalling is a novel target of oncogenic BRAF in metastatic melanoma. *Br J Cancer* 101:1448–55

Garbe C, Eigentler TK, Keilholz U *et al.* (2011) Systematic review of medical treatment in melanoma: current status and future prospects. *Oncologist* 16:5–24

Grishchuk Y, Ginet V, Truttmann AC *et al.* (2011) Beclin 1-independent autophagy contributes to apoptosis in cortical neurons. *Autophagy* 7:1115–31

Hill DS, Martin S, Armstrong JL *et al.* (2009) Combining the endoplasmic reticulum stress-inducing agents bortezomib and fenretinide as a novel therapeutic strategy for metastatic melanoma. *Clin Cancer Res* 15:1192–8

Hiscutt EL, Hill DS, Martin S *et al.* (2010) Targeting X-linked inhibitor of apoptosis protein to increase the efficacy of endoplasmic reticulum stress-induced apoptosis for melanoma therapy. *J Invest Dermatol* 130:2250–8

Howlett AC, Barth F, Bonner TI *et al.* (2002) International Union of Pharmacology. XXVII. Classification of cannabinoid receptors. *Pharmacol Rev* 54:161–202

Kabeya Y, Mizushima N, Ueno T *et al.* (2000) LC3, a mammalian homologue of yeast Apg8p, is localized in autophagosome membranes after processing. *EMBO J* 19:5720–8

Kimura S, Noda T, Yoshimori T (2007) Dissection of the autophagosome maturation process by a novel reporter protein, tandem fluorescent-tagged LC3. *Autophagy* 3:452–60

Massi P, Vaccani A, Bianchessi S *et al.* (2006) The non-psychoactive cannabidiol triggers caspase activation and oxidative stress in human glioma cells. *Cell Mol Life Sci* 63:2057–66

Maycotte P, Aryal S, Cummings CT *et al.* (2012) Chloroquine sensitizes breast cancer cells to chemotherapy independent of autophagy. *Autophagy* 8: 200–12

McGill A, Frank A, Emmett N *et al.* (2005) The anti-psoriatic drug anthralin accumulates in keratinocyte mitochondria, dissipates mitochondrial membrane potential, and induces apoptosis through a pathway dependent on respiratory competent mitochondria. *FASEB J* 19:1012–4

Michaud M, Martins I, Sukkurwala AQ *et al.* (2011) Autophagy-dependent anticancer immune responses induced by chemotherapeutic agents in mice. *Science* 334:1573–7

Pertwee RG (2008) The diverse CB1 and CB2 receptor pharmacology of three plant cannabinoids: delta9-tetrahydrocannabinol, cannabidiol and delta9-tetrahydrocannabivarin. *Br J Pharmacol* 153:199–215

Prieto PA, Yang JC, Sherry RM *et al.* (2012) CTLA-4 blockade with ipilimumab: long-term follow-up of 177 patients with metastatic melanoma. *Clin Cancer Res* 18:2039–47

Rosenfeldt MT, O'Prey J, Morton JP *et al.* (2013) p53 status determines the role of autophagy in pancreatic tumour development. *Nature* 504:296–300

Russell RC, Tian Y, Yuan H *et al.* (2013) ULK1 induces autophagy by phosphorylating Beclin-1 and activating VPS34 lipid kinase. *Nat Cell Biol* 15:741–50

Salazar M, Carracedo A, Salanueva IJ *et al.* (2009a) TRB3 links ER stress to autophagy in cannabinoid anti-tumoral action. *Autophagy* 5:1048–9

Salazar M, Carracedo A, Salanueva IJ *et al.* (2009b) Cannabinoid action induces autophagy-mediated cell death through stimulation of ER stress in human glioma cells. *J Clin Invest* 119:1359–72

Salazar M, Lorente M, Garcia-Taboada E *et al.* (2013) The pseudokinase tribbles homologue-3 plays a crucial role in cannabinoid anticancer action. *Biochim Biophys Acta* 1831:1573–8

Scarlatti F, Maffei R, Beau I *et al.* (2008) Role of non-canonical Beclin 1-independent autophagy in cell death induced by resveratrol in human breast cancer cells. *Cell Deth Differ* 15:1318–29

Shen HM, Codogno P (2011) Autophagic cell death: Loch Ness monster or endangered species? *Autophagy* 7:457–65

Shimizu K, Takahama S, Endo Y *et al.* (2012) Stress-inducible caspase substrate TRB3 promotes nuclear translocation of procaspase-3. *PloS One* 7:e42721

Shrivastava A, Kuzontkoski PM, Groopman JE *et al.* (2011) Cannabidiol induces programmed cell death in breast cancer cells by coordinating the cross-talk between apoptosis and autophagy. *Mol Cancer Ther* 10:1161–72

Takahashi A, Kimura T, Takabatake Y *et al.* (2012) Autophagy guards against cisplatin-induced acute kidney injury. *Am J Pathol* 180:517–25

Tomic T, Botton T, Cerezo M *et al.* (2011) Metformin inhibits melanoma development through autophagy and apoptosis mechanisms. *Cell Death Dis* 2:e199

Torres S, Lorente M, Rodriguez-Fornes F *et al.* (2011) A combined preclinical therapy of cannabinoids and temozolomide against glioma. *Mol Cancer Ther* 10:90–103

Velasco G, Sanchez C, Guzman M (2012) Towards the use of cannabinoids as antitumour agents. *Nat Rev Cancer* 12:436–44

White E (2012) Deconvoluting the context-dependent role for autophagy in cancer. *Nat Rev Cancer* 12:401–10

Wolchok JD, Neyns B, Linette G *et al.* (2010) Ipilimumab monotherapy in patients with pretreated advanced melanoma: a randomised, double-blind, multicentre, phase 2, dose-ranging study. *Lancet Oncol* 11:155–64

Yang ZJ, Chee CE, Huang S *et al.* (2011) The role of autophagy in cancer: therapeutic implications. *Mol Cancer Ther* 10:1533–41